Une telle variation de composition est confirmée par l'absence de taches de diffractions remplacées par des diffusions aux grands angles qui semblent traduire l'existence d'un désordre dans le précipité. Ce désordre entrainerait une variation dans la composition de la maille spinelle. Le précipité serait constitué de chaines ⟨110⟩ ordonnées, plus ou moins rapprochées les unes des autres selon la composition du précipité.

Le diagramme de diffraction aux grands angles se transforme bien vers 200 °C, les trainées de diffusion disparaissent lorsque la composition du précipité devient constante. C'est aussi à partir de 200 °C que la taille des précipités croît rapidement (Fig. 3). Jusqu'à 200 °C les cristaux contiennent moins d'une trentaine de mailles de structure spinelle ce qui explique probablement que leur composition soit mal définie.

L'évolution telle que nous venons de la décrire n'est évidemment qu'un schéma permettant de préciser le type de précipitation. Pour faire une description plus exacte il faudrait tenir compte de la variation de l'énergie de liaison de l'ion nickel avec la composition du précipité et de l'influence de l'énergie superficielle entre les deux phases; cette dernière doit être importante dans les premiers stades de l'agglomération.

Conclusion

L'étude d'un monocristal renfermant $1{,}8 \times 10^{-3}$ ions Ni^{2+} par molécule nous a permis de préciser le processus de précipitation après trempe qui se fait en deux étapes.

Par recuit à basse température il apparait une phase de composition mal définie et qui varie avec la température. On peut considérer que cette étape est une pré-précipitation: les agglomérats formés restent de petite taille et ne contiennent pas plus d'un millier d'ions de chaque signe. Par recuit ces cristaux s'enrichissent en nickel pour atteindre la composition de la phase stable à haute température Li_2NiF_4 vers 730 °C et grossissent ensuite. Au delà de cette température on peut véritablement parler de précipitation. Nous avons déterminé la composition de la solution solide à l'équilibre et mesuré l'énergie nécessaire pour faire passer l'ion Ni^{2+} d'une phase à l'autre: cette énergie très faible 0,05 eV explique la relativement grande solubilité du nickel dans le fluorure de lithium.

Références

BERGE, P., DUBOIS, M., BLANC, G. & ADAM-BENVENISTE, M. (1965). *J. de Phys.* **26**, 339.

JEHANNO, G. & PERIO, P. (1968). *Bull. Soc. franç. Minér. Crist.* A paraître.

LEVELUT, A. M., LAMBERT, M. & GUINIER, A. (1967). *C.r. Acad. Sci. Paris*, **255**, 319.

PETIAU, J. (1966). Thèse, Faculté des Sciences de Paris.

WYCKOFF, R. W. G. (1964). *Crystal Structures*, Vol. 2, Chap. 8. New York: Interscience Publishers.

Acta Cryst. (1968). A**24**, 464

Periodic Slip Processes and the Formation of Polytypes in Zinc Sulphide Crystals

BY S. MARDIX, Z. H. KALMAN AND I. T. STEINBERGER*

Department of Physics, Hebrew University, Jerusalem, Israel

(*Received* 24 *April* 1967 *and in revised form* 21 *December* 1967)

Inherent deformations of ZnS polytype regions are determined by measuring angles between linear markings. The deformations are correlated to the crystallographic structures of the polytypes as well. The relations clearly indicate that polytype formation occurred by a periodic slip process after crystal growth had been completed. Further observations substantiating this model are quoted.

Introduction

Various theories were put forward to explain the phenomenon of polytypism. Frank (1951) explained the formation of polytypes in silicon carbide by a growth mechanism around a screw dislocation. Frank's theory was improved by Mitchell (1957*a*,*b*) and Krishna & Verma (1965) to account for polytypism in silicon carbide and cadmium iodide.

Considering polytypes in ZnS, it was stated in previous publications (Lendvay & Kovács, 1966; Mardix & Steinberger, 1966; Daniels, 1966), that polytypes may be formed after growth by allotropic transformations governed by a periodic slip process. In this paper we show that this mechanism of allotropic transformation is the most common, if not the only, mechanism involved in polytype formation in ZnS.

Linear features appearing on a crystal's faces are investigated as to the correlation between their tilt plane, angle of tilt and the structure of the region on which they appear.

* On leave of absence at the Department of Chemistry, University of Southern California, Los Angeles, Calif. 90007, U.S.A.

This work deals only with experiments performed on polytypes of relatively low periodicity.

The crystals – general description

The crystals were grown from chemically pure zinc sulphide powder, in a quartz tube, by a method similar to that described by Patek (1961). Growth temperature was about 1250°C. During growth about one atm. of hydrogen sulphide was present in the tube.

The most common crystal habits were the platelet, rod, and whisker types. The present investigation was done mostly with platelets of approximately 50 microns thickness and a length of a few millimetres. Under suitable magnification, a great number of parallel striations can be seen on the platelets. These striations are the borderlines of regions of uniform birefringence (Brafman & Steinberger, 1966). The breadth of a region may reach up to 1 mm. X-ray photographs of the broader regions (*i.e.* >0·1 mm) showed that they are single crystals and thus have regular stacking sequence throughout the region. When viewed between crossed polarizers, each region appears coloured. Changes of colour are due to variation of birefringence from region to region. The external faces of different regions are generally not in one plane. All the crystals have a common threefold axis (*c* axis) in the direction of the crystal's length, which is perpendicular to the striations. The external faces are, in part, (11.0) or (1$\bar{1}$.0) planes; or higher index planes forming small angles with (11.0) or (1$\bar{1}$.0) faces.

On the faces of the crystals one may observe numerous lines approximately in the direction of the *c* axis (Fig. 1). The lines are, in part, the boundaries of partially completed layers (*b* in Fig. 1), or of secondary growth on the crystal's face (*c* in Fig. 1). We shall henceforth refer to them as 'linear markings'. Edges of the main faces of the platelets (*a* in Fig. 1) will also be included in this term.

The geometry of periodic slip processes

It is assumed that each specimen grew originally as a single crystal, having one of the close-packed structures (probably a single one throughout). The repeat distance along the *c* axis contains *n* layers. Polytypes were formed in the specimen at a later stage by a periodic slip process, *i.e.* a slip (within a certain crystallographic plane) which is periodically repeated every *m* structure layers throughout a macroscopic region of the specimen. In general *m* must be an integral multiple of *n*, otherwise nearest neighbour stacking order will be violated. This postulated slip mechanism may account for the formation of polytypes.

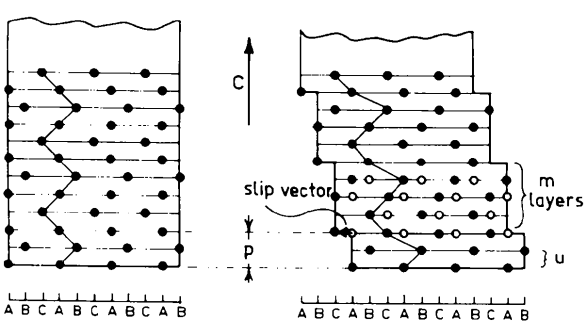

Fig. 2. The (11.0) plane of a ZnS crystal before and after p.s.p. has occurred. Full circles represent Zn atoms; empty circles represent Zn atoms at positions before slip has occurred.

For example the polytype 4*H* (2 2) transforms into 12*R* (3 1)$_3$ by a slip process of periodicity 4. Layer positions change by this process in the following way:

$$\begin{array}{l} ABACABACABACABAC\ldots \quad (4H) \\ \quad\downarrow \\ \quad CBCACBCACBCACB\ldots \\ \qquad\downarrow \\ \qquad BABCBABCBA\ldots \\ \qquad\quad\downarrow \\ \qquad\quad ACABAC\ldots \\ \qquad\qquad\downarrow \\ \qquad\qquad CB\ldots \end{array}$$

Positions in the final polytype are thus

$$ABCBCABABCACABCB\ldots \quad (12R)$$

This slip process generates slip bands of equal width $m \cdot u$ (u denotes the distance between two neighboring atomic layers) and constant slip height (see Fig. 2). This process is repeated throughout a macroscopic region of the specimen, and it thus follows that the polytype regions are, in general, macroscopically deformed with respect to the original crystal.

More than one periodic slip may successively occur in a given specimen.

In order to be operative in the formation of polytypes in close packed structures a periodic slip process must have the following properties:

(*a*) The slip plane must be perpendicular to the *c* axis.

(*b*) The slip vector must be one of the three 'cyclic' vectors

$$\mathbf{s}_1 = \frac{\mathbf{a}_1 - \mathbf{a}_2}{3} \qquad \mathbf{s}_2 = \frac{\mathbf{a}_2 - \mathbf{a}_3}{3} \qquad \mathbf{s}_3 = \frac{\mathbf{a}_3 - \mathbf{a}_1}{3} \qquad (1)$$

or one of the three anticyclic vectors $-\mathbf{s}_1$, $-\mathbf{s}_2$ or $-\mathbf{s}_3$. ($\mathbf{a}_1, \mathbf{a}_2, \mathbf{a}_3$ are the three unit vectors of the basal plane).

The polytype region resulting from a single periodic slip process (p.s.p.) will, in general, differ from the original sample both in internal structure and external shape.

The internal structure of the resulting polytype is uniquely determined by the structure of the original polytype, the periodicity of the slip and the height *p* of the slipped layer within the original unit cell. It can be seen from Fig. 2 that the sign of the slip vector is determined by *p*.

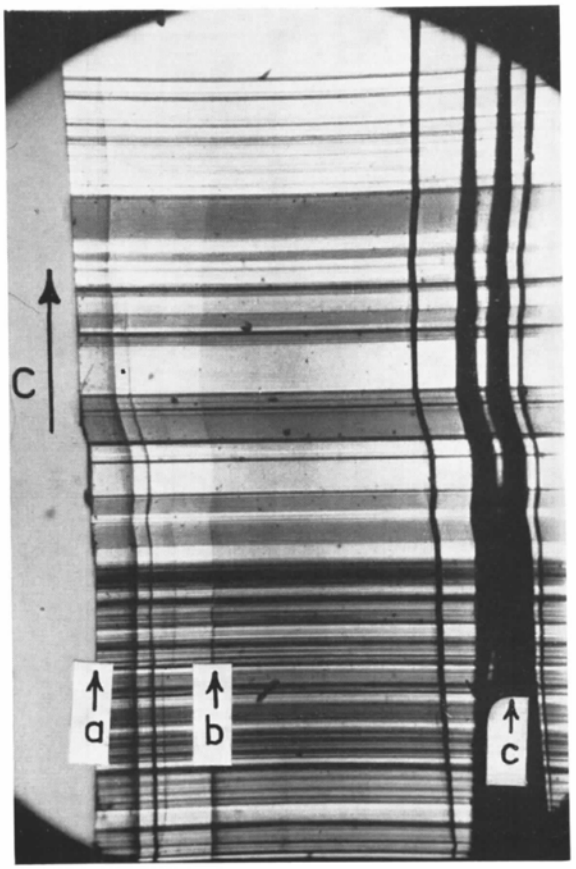

Fig. 1. Part of a ZnS platelet (×100) seen under partially crossed polarizers. Striated regions perpendicular to the *c* axis are polytypes. Lines in the general direction of the *c* axis are the linear markings referred to in the text.

[*To face p.* 465

The change in external shape is explained by regarding the p.s.p. as a homogeneous macroscopic shear deformation, which is determined by the slip vector **s** and the slip periodicity m. If more than one p.s.p. occurs in a given specimen, the process can be regarded as a succession of single periodic slips.

As various different polytype regions result from one original structure, it is necessary to distinguish between a certain polytype and its twin. This will be accomplished by writing the Hägg symbol (Hägg, 1943) in such a way that the first sign is always +, or in the Zhdanov symbol, by agreeing the first number to denote always a cyclic order. Also in this work twins of the cubic structure will be denoted in the Zhdanov symbol by (n 0) or (0 n) respectively. The definition of cyclic and anticyclic sense has to be the same for all polytype regions throughout a given specimen. For each specimen the sense can be chosen arbitrarily as the difference between a certain polytype and its twin is that of an ordinary rotation.

A simple p.s.p. will be denoted as follows:

$$\pm \mathbf{s}_i(p,m) \,.\, (Z) \tag{2}$$

where $+\mathbf{s}_i$ or $-\mathbf{s}_i$ denotes the slip vector, p the height of the slipped plane and m the periodicity of the slip. Z symbolizes Hägg's notation for the original polytype. Obviously the value of p (for a given p.s.p.) depends on the way Hägg's symbol is written. The operation of the p.s.p. in this case is formally obtained by changing the pth sign in the symbol, *i.e.*

$$-\mathbf{s}_i(2,4) \,.\, (++--) = (+---) \,.$$

Another example:

$$+\mathbf{s}_i(3,8) \,.\, (++--++--) = (+++-++--) \,.$$

The equivalent Zhdanov notation would be

$-\mathbf{s}_i(2,4) \,.\, (22) \rightarrow (13)$

$+\mathbf{s}_i(3,8) \,.\, (22) \rightarrow (3122)$ respectively .

The macroscopic deformation caused by a p.s.p. is a shear deformation, and it will be assumed that the slip does not affect the value u, *i.e.* the distance between neighboring atomic c planes. Let $\mathbf{r}$ denote a position vector of a volume element in the undeformed material, and $\mathbf{r}'$ the position vector of the same element after deformation. Let $\mathbf{a}_1$, $\mathbf{a}_2$ and $\mathbf{c}_0$ denote a hexagonal system of axes. Let the unit cell of the undeformed region contain n atomic layers in the $\mathbf{c}$ direction, (thus $c_0 = n \,.\, u$) and assume that J periodic slips have been operative, each characterized by its slip vector $\mathbf{s}_i$ and its periodicity m_i (the height p_i within the unit cell does not affect the macroscopic deformation).

$$\left.\begin{aligned} \mathbf{r} &= x_1\mathbf{a}_1 + x_2\mathbf{a}_2 + y\mathbf{c}_0 \\ \mathbf{r}' &= x_1\mathbf{a}_1 + x_2\mathbf{a}_2 + y(\mathbf{c}_0 + \mathbf{S}) \end{aligned}\right\} \tag{3}$$

where

$$\mathbf{S} = \sum_{i=1}^{j} \frac{\mathbf{s}_i}{m_i} \tag{4}$$

and

$$\mathbf{s}_i = \frac{\sigma_{i1}\mathbf{a}_1 + \sigma_{i2}\mathbf{a}_2}{3} \,. \tag{5}$$

From the definition (1) it can be seen that the values of σ_{i1} and σ_{i2} are ± 1 or ± 2 so that

$$\sigma_{i1} + \sigma_{i2} = 0 \bmod 3 \,.$$

From (4) and (5) we have

$$\mathbf{S} = \mu_1\mathbf{a}_1 + \mu_2\mathbf{a}_2 \,. \tag{6}$$

μ_1 and μ_2 are in general not integers and are readily calculated from the slip vectors $\mathbf{s}_i$.

Thus

$$\mathbf{r}' = (x_1 + y\mu_1)\mathbf{a}_1 + (x_2 + y\mu_2)\mathbf{a} + y\mathbf{c}_0 \,. \tag{7}$$

From the conditions imposed on the magnitude and directions of the slip vectors and their periodicity m it follows that the deformed material is again a crystal and that any crystallographic direction (or plane) in the original lattice deforms into another crystallographic direction (or plane) in the new lattice.

A simple relation exists between the projections of $\mathbf{r}$ and $\mathbf{r}'$ upon a plane π, containing the c axis and the slip s. Let $\boldsymbol{\varrho}$ and $\boldsymbol{\varrho}'$ respectively denote the projection of $\mathbf{r}$ and $\mathbf{r}'$ upon π, and let $\mathbf{V}_c$ and $\mathbf{V}_s$ denote respectively the unit vectors in the direction of the c axis and the slip $\mathbf{S}$. $\mathbf{V}_c$ and $\mathbf{V}_s$ are mutually perpendicular.

Then

$$\left.\begin{aligned} \boldsymbol{\varrho} &= (\mathbf{r} \,.\, \mathbf{V}_c)\mathbf{V}_c + (\mathbf{r} \,.\, \mathbf{V}_s)\mathbf{V}_s \\ \boldsymbol{\varrho}' &= (\mathbf{r}' \,.\, \mathbf{V}_c)\mathbf{V}_c + (\mathbf{r}' \,.\, \mathbf{V}_s)\mathbf{V}_s \end{aligned}\right\} \,. \tag{8}$$

From equation (3)

$$\left.\begin{aligned} r \,.\, \mathbf{V}_c &= \mathbf{r}' \,.\, \mathbf{V}_c = yc_0 \\ \mathbf{r}' \,.\, \mathbf{V}_s &= \mathbf{r} \,.\, \mathbf{V}_s + yS \end{aligned}\right\} \,, \tag{9}$$

where

$$S = |\mathbf{S}| \quad \text{and} \quad c_0 = |\mathbf{c}_0| \,.$$

Let α denote the angle between $\boldsymbol{\varrho}$ and the c axis, and β the angle between $\boldsymbol{\varrho}'$ and the c axis [Fig. 3(*b*)]

$$\left.\begin{aligned} \varrho \cos\alpha &= \boldsymbol{\varrho} \,.\, \mathbf{V}_c = \mathbf{r} \,.\, \mathbf{V}_c \\ \varrho \sin\alpha &= \boldsymbol{\varrho} \,.\, \mathbf{V}_s = \mathbf{r} \,.\, \mathbf{V}_s \end{aligned}\right\} \,. \tag{10}$$

From equation (9)

$$\operatorname{tg}\alpha = \mathbf{r} \,.\, \mathbf{V}_s / yc_0 \,.$$

Similarily, using equation (9)

$$\operatorname{tg}\beta = \boldsymbol{\varrho}' \,.\, \mathbf{V}_s / \boldsymbol{\varrho}' \,.\, \mathbf{V}_c = \frac{\mathbf{r} \,.\, \mathbf{V} + yS}{yc_0} \,.$$

Thus

$$\operatorname{tg}\beta - \operatorname{tg}\alpha = S/c_0 \,. \tag{11}$$

Relation (11) depends only on the slip $\mathbf{S}$; thus within any region characterized by a given total slip $\mathbf{S}$, $\operatorname{tg}\beta - \operatorname{tg}\alpha = \text{constant}$ holds for every direction $\mathbf{r}$. It should be noted that neither $\mathbf{r}$ nor $\mathbf{r}'$ needs to be a crystallographically significant direction. The derivation de-

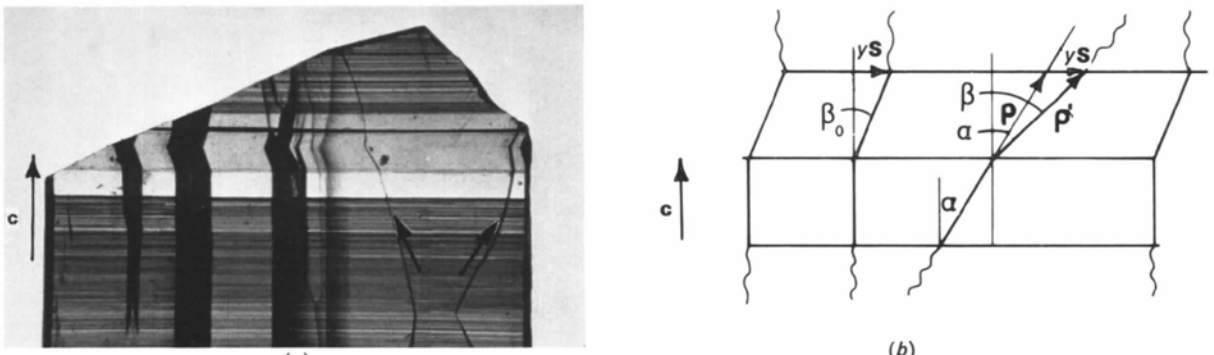

Fig. 3. (*a*) Linear markings of types I and II. Type I have segments in some regions parallel to the *c* axis. The two markings of type II are indicated by arrows. (*b*) Notation employed for kink angles. Tilt plane lies in the plane of the drawing.

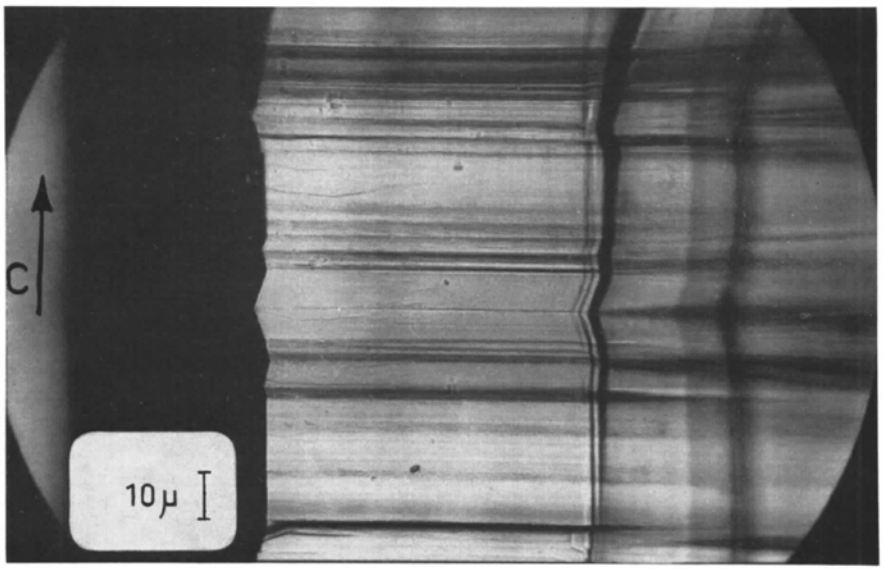

Fig. 4. Linear markings on narrow regions.

[*To face p.* 466

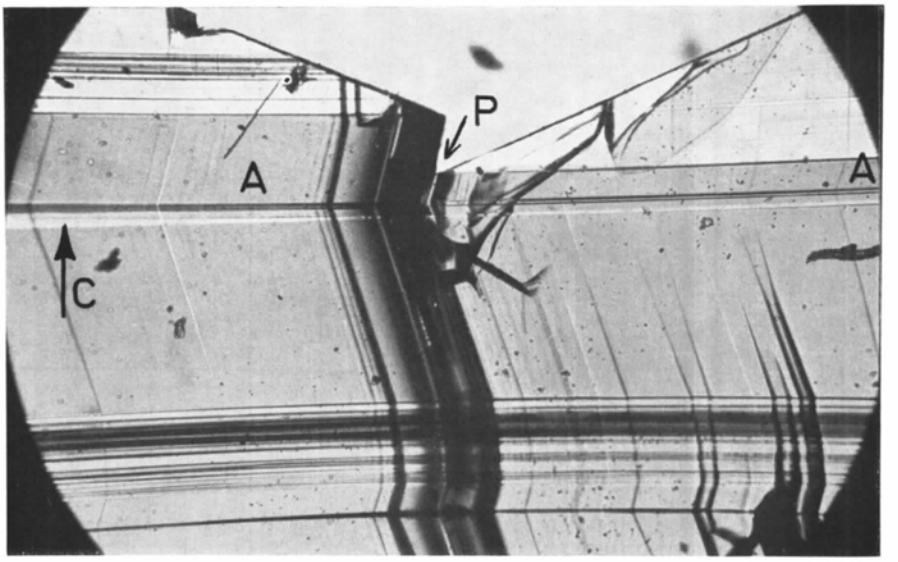

(*a*)

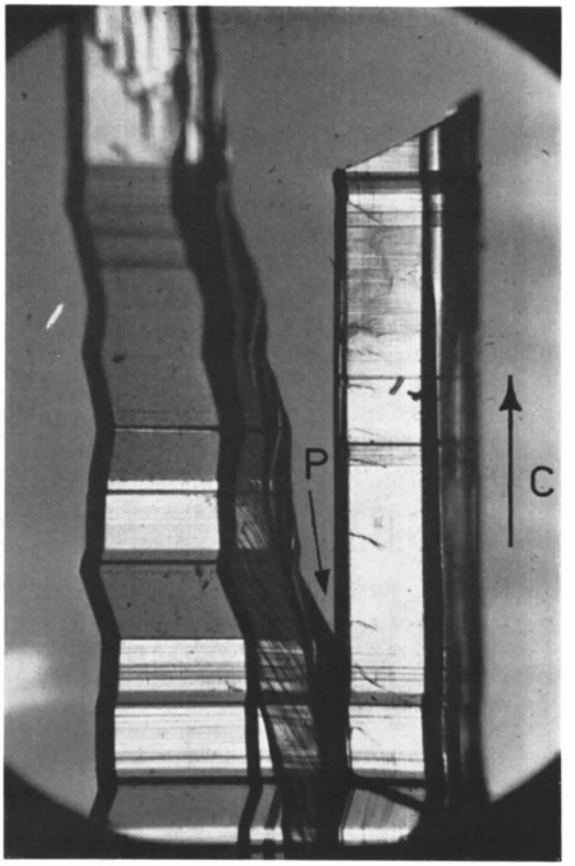

(*b*)

Fig. 5. (*a*) & (*b*) Polytype regions in cracked crystals (× 100).

pends solely on the periodicity of the slip process. In fact, satisfaction of (11) for several **r** values proves that periodic slip has occurred.

Experimental

It is appropriate to start with the fundamental observation that for each uniform region (accessible to measurement) there exist several easily recognizable, but different directions **r**, all yielding the same **S** value.

In fact, the linear markings on the crystal faces, which were determined above, yield readily measurable **r** directions. They resolve (*e.g.* Fig. 1) under magnification into a zigzag pattern composed of straight segments. Some of these patterns run parallel to each other, but this is certainly not true for all of them. All of the segments mentioned are straight lines within a structurally homogeneous region, but all markings become kinked on the interface of two neighbouring regions. These facts indicate that the markings were originally straight lines throughout the entire specimen. At some later stage, *e.g.* during the cooling down period of the crystal, p.s. processes had occurred, creating the various polytype regions and simultaneously deforming the linear markings into the observed zigzag pattern. The occurrence of slip will be based on measurements of kink angles and on the fact that for a given interface different markings give the same **S**, by using (11). The values of **S** will be demonstrated to be such as are consistent with a periodic slip, homogeneous down to atomic scale. Finally, the p.s.p. will be shown to account for the polytype structure as determined by X-ray methods.

Measurements of kink angles and tilt planes

Angles were measured between each straight line segment and the **c** direction common to all regions.

Measurements were performed on a 'Standard Universal' Zeiss microscope. Specimens were mounted on a device permitting the crystals to be tilted about their *c* axis. The tilting device was placed on the standard rotating stage. The angles between two adjoining straight line segments were obtained by adjusting crystal and magnification so that considerable parts of two regions filled the field of view. In order to measure angles α and β defined in equation (10), the plane π pertaining the two regions has to be normal to the direction of view. This was done by first selecting kinks which had one of their segments parallel to the *c* axis (kinks of type I in Fig. 3). The crystal was then tilted until the plane containing both segments (the tilt plane) lay parallel to the direction of view (*i.e.* both segments appeared as one straight line). Tilting now the specimen by 90° about its *c* axis permits directly the measurement of the tilt angle β_0. Next angles α and β between segments of Type II (none parallel to the **c** direction) and *c* axis were measured without changing the orientation of the specimen. The maximum overall error in measuring each angle was about 20′. This procedure was repeated for different pairs of regions.

It was found that all kinks both of type I and II lying at an interface between two given regions obey the relation $\mathrm{tg}\,\beta - \mathrm{tg}\,\alpha = \mathrm{tg}\,\beta_0 = \text{constant}$ (for a given interface). The values of both α and β ranged practically from $+90°$ to $-90°$, and except for a steady preference of the value $\alpha = 0$ no regularity in the abso-

Table 1. *Periodic slip processes indicated by results from zinc sulphide specimens*

Specimen no. & region	α (°)	Tilt plane	Structure	Postulated original structure	P.S.P. consistent with α, tilt plane and structure	Calc. α (°)
212/51						
a	0	—	2*H* (1 1)	2*H* (1 1)	—	—
b	19·2	($\bar{2}$1.0)	3*C* (2 0)	2*H* (1 1)	$\mathbf{s}_1(2,2)$	19·47
c	19·4	(11.0)	3*C* (0 2)	2*H* (1 1)	$-\mathbf{s}_3(1,2)$	19.47
d	0	—	8*H* (4 4)	—	—	—
180/52						
a	19·7	($\bar{2}$1.0)	3*C* (0 4)	4*H* (2 2)	$-\mathbf{s}_1(1,4)-\mathbf{s}_1(2,4)$	19·47
b	0	—	4*H* (2 2)	—	—	—
c	19·8	($\bar{2}$1.0)	3*C* (4 0)	4*H* (2 2)	$\mathbf{s}_1(3,4)+\mathbf{s}_1(4,4)$	19·47
d	17·0	(10.0)	4*H* (2 2)	4*H* (2 2)	$\mathbf{s}_1(3,4)-\mathbf{s}_3(3,4)$	17·033
e	19·0	($\bar{2}$1.0)	3*C* (4 0)	4*H* (2 2)	$\mathbf{s}_1(3,4+\mathbf{s}_1(4,4)$	19·47
f	28·3	(1$\bar{2}$.0)	4*H* (2 2)	4*H* (2 2)	$\mathbf{s}_1(3,4)-\mathbf{s}_2(3,4)$ $+\mathbf{s}_3(3,4)-\mathbf{s}_2(3,4)$	27·93
203/56						
a	6·5	($\bar{2}$1.0)	18*R* (4 2)$_3$	6*H* (3 3)	$\mathbf{s}_1(4,6)$	6·73
b	6·4	($\bar{2}$1.0)	18*R* (2 4)$_3$	6*H* (3 3)	$-\mathbf{s}_1(3,6)$	6·73
c	0	—	6*H* (3 3)	—	—	—
d	11·3	(1$\bar{1}$.0)	3*C* (6 0)	6*H* (3 3)	$\mathbf{s}_2(4,6)+\mathbf{s}_2(5,6)$ $+\mathbf{s}_3(6,6)$	11·53
e	0	—	6*H* (3 3)	—	—	—
f	11·3	(1$\bar{1}$.0)	3*C* (0 6)	6*H* (3 3)	$-\mathbf{s}_2(4,6)-\mathbf{s}_2(5,6)$ $-\mathbf{s}_3(6,6)$	11·53
g	0	—	6*H* (3 3)	—	—	—
h	11·3	(01.0)	3*C* (0 6)	6*H* (3 3)	$-\mathbf{s}_1(3,6)-\mathbf{s}_3(2,6)$ $-\mathbf{s}_3(1,6)$	11·53

lute value of the angles α was detected. Table 2 gives a number of representative values measured.

Table 2. *Kink angles*

Crystal no.	Linear marking	α	β	tg β − tg α
180/5	1	0·0°	19·1°	0·346
	2	−65·5	−61·5	0·350
	3	19·0	34·4	0·341
	4	−10·5	9·4	0·351
175/21	1	−0·6	5·5	0·106
	2	3·2	9·7	0·115
	3	−1·8	4·5	0·110
	4	19·2	24·4	0·106
232/76	1	−0·2	15·6	0·281
	2	7·0	24·0	0·322
	3	−8·3	7·9	0·284
	4	−10·9	7·5	0·324
	5	8·3	23·0	0·302
	6	0·6	16·7	0·290

The indices of the tilt plane (which is always a crystallographic plane) were determined by means of small amplitude (5°) oscillation photographs. Results are tabulated in columns 2 and 3 of Table 1.

Structure determination

The structure of each region within a given specimen was determined by *c*-axis oscillation photographs, with the use of a Hilger microbeam X-ray generator (Cu *K* radiation) and a standard oscillation camera ($r = 30$ mm, 15° oscillation) having a fine collimator (dia. 0·1 mm). Usable photographs were obtained when up to three different regions were simultaneously in the beam, as reflexion from different regions could be distinguished by the shape of the spots. All regions of a given specimen were obtained by oscillating the crystal about the same orientation. This permits the determination of both structure and relative orientation (within the required limits) of each region. Note in this respect that the oscillation photograph of a certain polytype and its twin are in general different: the positions of the spots are inverted with respect to the zero-layer.

Structures of the various regions were determined by comparing measured intensities with those calculated for the postulated structures, as previously reported (Mardix, Alexander, Brafman & Steinberger, 1967). Results appear in column 4, Table 1.

Conclusions and discussion

Results similar to those in Table 1 were obtained from about 10 different specimens with 3–15 regions measured on each crystal.

In all of these regions both external deformation and internal structure were found to fit in the same way as those of the three samples cited in the tables.

From the results two separate conclusions may be drawn: First the constancy of the differences tg α − tg β (of the straight segments) for two adjoining regions indicates that a homogeneous shear deformation has occurred within each region. The fact that each deformed region is again a single crystal of close packed structure indicates that the shear deformation is homogeneous down to atomic scale, *i.e.* that the deformation was due to periodic slip processes. Furthermore, since the linear surface markings utilized (*e.g.* secondary growths) are formed only during the last stages of the crystal growth, deformation must have occurred after the growth process was completed, or almost completed.

The inherent relationship between the periodic slip process and the generation of polytypes is clearly manifested by comparing the crystallographic structures of two adjoining regions in view of the slip vector obtained from the shear deformation. The same periodic slip process explains the observed structures, orientations and shear deformation. Polytype formation by periodically recurring slip is thus fully substantiated for all regions which were wide enough (>0·1 mm) for the X-ray probe. Actually, it was possible to distinguish zigzag patterns of the linear features also in much narrower regions (Fig. 4) without measuring kink angles. X-ray measurements of such conglomerations showed these to be actually composed of various polytypes. These polytypes showed the same periodicities as those appearing in the wider region. Additional evidence may be seen in Fig. 5. These figures are micrographs of single-crystal platelets as seen between partially crossed polarisers.

In Fig. 5(*a*) a cubic region *A* can be seen which passes throughout the entire width of the crystal. (This region is tilted as mentioned above.) However, it may be observed that above point *P* where contact between the left and right part of the crystal is interrupted, the cubic phase continues in the left part only, whilst the right part shows a different structure. In other words above point *P* only the left part underwent transformation.

A similar situation prevails in the cracked crystal shown in Fig. 5(*b*), where above point *P* the two parts of the crystal show different structure, whilst below *P* the same structure holds throughout the width of the crystal.

As the cracks in the crystals formed after completion of growth, these observations may be regarded as proof to the postulated mode of polytype formation discussed above.

In this work only polytypes of relatively short periods have been measured. In longer period polytypes transformations by a small number of p.s.p. result in small kink angles, thus requiring higher measuring accuracy than possible with the apparatus employed. On the other hand for structures (of high periodicity) showing larger kink angles, the number of possible p.s.p. becomes too large to describe the transformation meaningfully. Nevertheless a few higher-period-polytype angles could also be determined and compared

to the structures, in complete agreement with the above model.

It should be noted that structure transformation by periodic slip processes from a hexagonal structure will always result in polytypes of even periodicity. As all polytypes identified in this laboratory (more than 60; Steinberger & Mardix, 1967) were of even periodicity, it is safe to assume that all these were derived from the $2H$ hexagonal phase. This assumption is in full accord with the high ($\sim$1250°C) growth temperature.

Two further observations have to be quoted here because of their relevance to the model. First, in a given crystal specimen all the polytypes are closely related (Mardix *et al.*, 1967); this fact is in full accord with the assumption that the polytypes have been created by periodic slip from the same parent structure. The second observation deals with the transformation process itself; it has been shown (Mardix & Steinberger, 1966; Steinberger & Mardix, 1967) that by applying moderate pressure by a knife edge polytypes can be transformed even at room temperature. Simultaneously, macroscopic tilt angles are induced.

This work dealt only with the essentially geometrical description of polytype formation. Discussion of the underlying physical processes seems to be still too speculative, though little doubt can exist about the fundamental role of dislocations. It should be noted in this connexion that the transformation $2H \rightarrow$cubic was directly observed (d'Aragona, 1966) to be due to the expansion of partials.

References

Brafman, O. & Steinberger, I. T. (1966). *Phys. Rev.* **143**, 501.

Daniels, B. K. (1966). *Phil. Mag.* **14**, 487.

D'Aragona, F. S., Delavignette, P. & Amelinckx, S. (1966). *Phys. Stat. Sol.* **14**, K115.

Frank, F. C. (1951). *Phil. Mag.* **42**, 1014.

Hägg, G. (1943). *Ark. Kemi, Mineral. Geol.* **16B**, 1.

Krishna, P. & Verma, A. R. (1965). *Z. Kristallogr.* **121**, 36.

Landvay, E. & Kovàcs, P. (1966). *Act. Phys. Hung.* **20**, 31.

Mardix, S., Alexander, E., Brafman, O. & Steinberger, I. T. (1967). *Acta Cryst.* **22**, 808.

Mardix, S. & Steinberger, I. T. (1966). *Israel J. Chem.* **3**, 243.

Mitchell, R. S. (1957). *Z. Kristallogr.* **108**, 341.

Mitchell, R. S. (1957). *Z. Kristallogr.* **109**, 1.

Patek, K. (1961). *Czech. J. Phys.* **11**, 686.

Steinberger, I. T. & Mardix, S. (1967). *Proc. Intern. Conf.* II–VI *Semiconducting Compounds*, Brown Univ. Providence, Rhode Island. Benjamin Press.

Acta Cryst. (1968). A**24**, 469

Determination of Thermal Expansion of Germanium, Rhodium, and Iridium by X-rays

By H. P. Singh

Department of Physics, Banaras Hindu University, Varanasi-5, India

(*Received* 5 *February* 1968)

The lattice parameters of germanium, rhodium, and iridium were measured with a Unicam 19 cm high-temperature powder camera; the following equations represent the results:

$$\text{Ge: } a_t = 5{\cdot}6569 + 34{\cdot}22 \times 10^{-6}t + 10{\cdot}17 \times 10^{-9}t^2 - 0{\cdot}66 \times 10^{-12}t^3$$
$$\text{Rh: } a_t = 3{\cdot}8026 + 29{\cdot}27 \times 10^{-6}t + 10{\cdot}49 \times 10^{-9}t^2 + 0{\cdot}54 \times 10^{-12}t^3$$
$$\text{Ir: } a_t = 3{\cdot}8383 + 23{\cdot}52 \times 10^{-6}t + 4{\cdot}92 \times 10^{-9}t^2 + 0{\cdot}89 \times 10^{-12}t^3$$

Thermal expansion coefficients and Grüneisen parameters were also calculated.

Introduction

Experimental data on the thermal expansion of germanium, rhodium, and iridium at high temperatures are very scarce. The available data either refer to low temperatures or give the mean value at high temperatures measured over large intervals. In the case of germanium macroscopic measurements have been made by Dennis (1928) in the range 20 to 400°C. Straumanis & Aka (1952) made X-ray measurements for a very short range between 10 to 50°C. Nitka (1937) has determined the thermal expansion of 99·9% pure germanium by measuring the lattice parameters only at four temperatures from 20 to 840°C. His room-temperature lattice parameter value differs from that of Straumanis & Aka (1952) by about 0·002 Å.

The macroscopic thermal expansion coefficients of rhodium at high temperatures have been determined by Ebert (1938) and those of iridium by Holborn & Valentiner (1907). No X-ray measurements are available for either of these metals. Owing to this lack of data, it was thought desirable to measure the lattice parameters of these three metals in detail at high temperatures. Results of measurements are reported in this paper.

Experimental

Germanium, rhodium, and iridium were 'Specpure' powder which were filled in quartz capillaries of inner diameter 0·5 mm and annealed. Photographs were taken with a Unicam 19 cm diameter high-temperature powder camera in more than two sets. The camera was